ISSN 0021-3640, JETP Letters, 2019, Vol. 109, No. 6, pp. 398–403. © Pleiades Publishing, Inc., 2019.
Russian Text © The Author(s), 2019, published in Pis'ma v Zhurnal Eksperimental'noi i Teoreticheskoi Fiziki, 2019, Vol. 109, No. 6, pp. 401–407.

CONDENSED MATTER

Beats of Quantum Oscillations of the Resistance in Two-Subband Electron Systems in Tilted Magnetic Fields

A. A. Bykov[a, b, *], I. S. Strygin[a], A. V. Goran[a], I. V. Marchishin[a], D. V. Nomokonov[a], A. K. Bakarov[a], S. Albedi[c], and S. A. Vitkalov[c]

[a] *Rzhanov Institute of Semiconductor Physics, Siberian Branch, Russian Academy of Sciences, Novosibirsk, 630090 Russia*
[b] *Novosibirsk State University, Novosibirsk, 630090 Russia*
[c] *Physics Department, City College of the City University of New York, 10031 NY, USA*
**e-mail: bykov@isp.nsc.ru*

Received December 5, 2018; revised January 18, 2019; accepted January 22, 2019

Electron transport in single GaAs quantum wells of widths from 22 to 46 nm with two populated quantum-confinement subbands E^S and E^{AS} is investigated at a temperature of $T = 4.2$ K in tilted magnetic fields $B <$ 2 T. The angle α between the applied magnetic field and the normal to the plane of the structure under study is varied from 0° to 90°. In a perpendicular magnetic field ($\alpha = 0$), magnetointersubband oscillations with a period determined by the relation $\Delta_{SAS} = E^{AS} - E^S = j\hbar\omega_c$, where ω_c is the cyclotron frequency and j is a positive integer, are observed in all investigated quantum wells. In tilted fields, the peaks of magnetointersubband oscillations are shifted toward higher fields $B\cos\alpha$. This shift is explained by an increase in the energy splitting Δ_{SAS} with increasing component $B\sin\alpha$. In 46- and 36-nm-wide quantum wells, beats of magnetointersubband oscillations are observed at angles $\alpha > 72°$ and $\alpha > 85°$, respectively. The origin of this unexpected behavior of magnetointersubband oscillations in tilted magnetic fields is discussed.

DOI: 10.1134/S0021364019060080

Two types of quantum oscillations are prominent in the magnetoresistance of high-mobility quasi-two-dimensional systems with several populated energy subbands. One is the well-known Shubnikov–de Haas (SdH) oscillations: the resistance oscillates upon the variation of a magnetic field B perpendicular to a quasi-two-dimensional system as successive Landau levels cross the Fermi level E_F. In electron systems with two populated quantum-confinement subbands E^S and E^{AS} placed in the magnetic field, each subband features its own ladder of Landau levels, which leads to the appearance of two series of SdH oscillations. Since the difference of electron densities in the subbands is determined by the energy splitting $\Delta_{SAS} = E^{AS} - E^S$, it can be found by Fourier analysis from the difference between the frequencies of SdH oscillations with the inverse magnetic field. If $\varepsilon_F = [E_F - (E^S + E^{AS})/2] \gg \Delta_{SAS}$, SdH oscillations in weak magnetic fields experience beats, and the value of Δ_{SAS} can be determined from the positions of the beating nodes [1, 2].

Other resistance oscillations that result from the quantization of the electron orbital motion in a magnetic field are magnetointersubband (MIS) oscillations [3–6]. They occur owing to the elastic intersubband scattering of electrons, which becomes resonant upon the crossing of Landau levels belonging to different subbands. In systems with two subbands, such crossings take place when

$$\Delta_{SAS} = j\hbar\omega_c, \quad (1)$$

where j is a positive integer, $\omega_c = eB/m^*$ is the cyclotron frequency, and m^* is the electron effective mass. The peak positions of MIS oscillations in a perpendicular magnetic field are determined by Eq. (1). Similar to SdH oscillations, MIS oscillations are periodic in the inverse magnetic field, but, in contrast to the former, they are not suppressed by the temperature broadening of the Fermi distribution function. For this reason, MIS resistance oscillations are widely used to study quantum transport in the temperature range where SdH oscillations are already suppressed, i.e., $\hbar\omega_c \ll k_BT$ [7–15].

The impact of the in-plane component of a tilted magnetic field $\mathbf{B} = (B_x, 0, B_z)$ on the behavior of SdH oscillations in an electron system with two subbands in the case of $\varepsilon_F \gg \Delta_{SAS}$ was experimentally and theoretically investigated in [1, 2]. It was established that the in-plane component $B_x = B\sin\alpha$ shifts the nodes of the beat pattern to higher out-of-plane magnetic field

components $B_z = B\cos\alpha$, where α is the angle between the vector **B** and the normal to the plane of the quasi-two-dimensional system. The experimental results obtained were explained by an increase in Δ_{SAS} with B_x.

The influence of the tilted magnetic field $\mathbf{B} = (B_x, 0, B_z)$ on the energy spectrum of electrons in the potential $V(z)$ is described by the Hamiltonian [16]

$$H = \hbar^2 k_x^2/2m^* + e^2 B_z^2 x^2/2m^* + \hbar^2 k_z^2/2m^* + V(z) + e^2 B_x^2 z^2/2m^* - e^2 B_x B_z xz/m^*. \quad (2)$$

The first four terms in this Hamiltonian describe electrons in the out-of-plane magnetic field component B_z, while the last two terms appear owing to the presence of the in-plane component B_x. In a two-subband system, the dependence of the Landau level energies $E_N^{S,AS}$ on the magnetic field B_z is given by the expression

$$E_N^{S,AS} = \hbar\omega_{cz}(N + 1/2) - (+)\Delta_{SAS}/2, \quad (3)$$

where $\omega_{cz} = eB_z/m^*$ and N is the Landau level index.

The solution of Eq. (2) for the case of two parallel two-dimensional layers of zero thickness in a tilted magnetic field yields the intersubband splitting [2, 17]

$$\Delta_{SAS} = \Delta_{SAS}^0(1+\gamma^2)^{1/2}(2/\pi)E(\gamma/(1+\gamma^2)^{1/2}). \quad (4)$$

Here, Δ_{SAS}^0 is the intersubband splitting in zero magnetic field; $\gamma = \hbar\omega_{cx}k_F d/\Delta_{SAS}^0$, where $\omega_{cx} = eB_x/m^*$, d is the distance between the two-dimensional layers, and k_F is the Fermi quasimomentum; and $E(\gamma/(1+\gamma^2)^{1/2})$ is the complete elliptic integral of the first kind. Relation (4) is valid in the case of weak B_z, where $\hbar\omega_{cz} \ll \Delta_{SAS}^0$ and the effects of magnetic breakdown can be disregarded [2]. In this approximation, Δ_{SAS} depends only on the in-plane component B_x and increases with it, which is in full agreement with the experimental results reported in [1]. However, even for $B_z = 0$, Eq. (4) is valid only when the magnetic length is $(\hbar/eB_x)^{1/2} > d/2$ [1, 2].

Currently, experimental studies of the electron energy spectrum in quasi-two-dimensional systems in tilted magnetic fields mostly involve SdH oscillations and the quantum Hall effect [1, 16, 17]. However, it was recently shown that MIS oscillations can be used in such studies [18], since the positions of their peaks in a magnetic field are determined by intersubband energy splittings. One of the advantages of MIS oscillations in comparison with SdH oscillations and quantum Hall effect is that they allow studies of quantum transport in weak magnetic fields. Still, the behavior of MIS oscillations in tilted magnetic fields remains poorly investigated [18–20]. In this work, we further

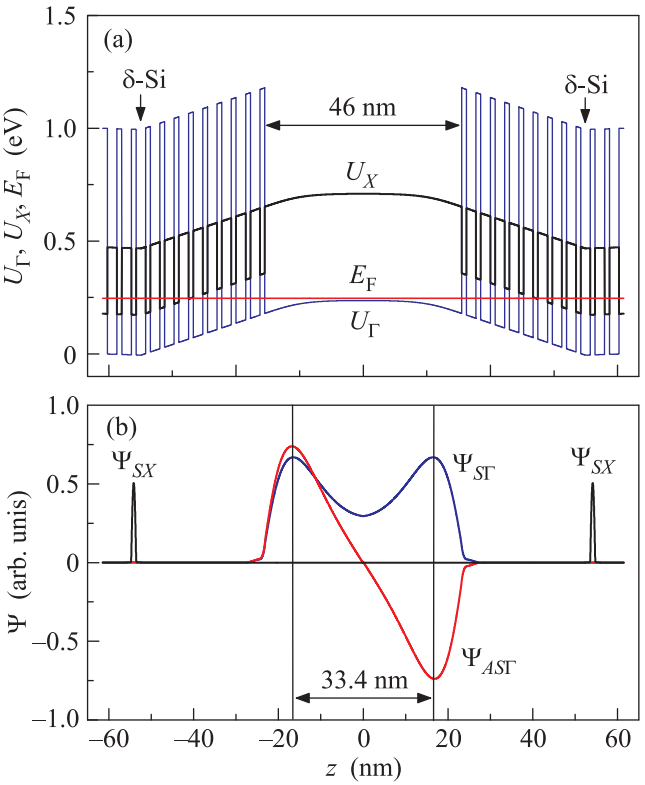

Fig. 1. (Color online) (a) Self-consistent calculation of the confining potentials $U_\Gamma(z)$ and $U_X(z)$ and the position of the Fermi level E_F for a wide GaAs quantum well and AlAs/GaAs superlattice side barriers. Arrows indicate the δ-doped layers. (b) Wavefunctions of Γ electrons occupying E^S and E^{AS} subbands in a GaAs quantum well of width $d_W = 46$ nm and of X electrons in the E^S subband in AlAs quantum wells near the δ-doped layers.

study the features of quantum transport of electrons in systems with two subbands in tilted magnetic fields by measuring MIS oscillations. One of the goals of our work is the experimental study of the dependence of Δ_{SAS} on the magnitude of the in-plane component of the titled magnetic field in single GaAs quantum wells of different widths.

We investigated symmetrically doped GaAs quantum wells with widths of 46, 36, 30, and 22 nm. Short-period AlAs/GaAs superlattices were used as barriers of the quantum wells [21, 22]. The results of self-consistent calculations of the confinement potentials U_Γ and U_X and electron wavefunctions for the 46-nm quantum well are shown in Fig. 1. The heterostructures were grown by molecular-beam epitaxy on GaAs (100) substrates. Samples for magnetotransport measurements represented Hall bars with a length of $L = 450$ μm and a width of $W = 50$ μm.

Measurements were carried out at $T = 4.2$ K in magnetic fields $B < 2$ T for different angles α between the normal to the plane of the quantum well and the

Table 1. Parameters of the samples: d_W is the width of the quantum well; n_T is the total electron density; n_S and n_{AS} are the electron densities in the first and second subbands, respectively; μ_y is the net electron mobility; Δ_{SAS}^{exp} and Δ_{SAS}^{theo} are the energy splittings determined from the period of MIS oscillations and obtained from a self-consistent calculation, respectively

Sample no.	d_W (nm)	n_T (10^{15} m^{-2})	n_S (10^{15} m^{-2})	n_{AS} (10^{15} m^{-2})	μ_y (m^2/(V s))	Δ_{SAS}^{exp} (meV)	Δ_{SAS}^{theo} (meV)
1	46	8.4	4.4	4.0	153	1.44	1.3
2	36	8.4	4.9	3.5	162	4.76	4.6
3	30	6.8	4.8	2.0	255	9.95	10.9
4	22	10	8.1	1.9	121	21.7	23.3

magnetic field. The angle was varied by rotating the sample along the longitudinal axis of the Hall bar; thus, only the magnetic-field components B_z and B_x were varied during the measurements. Resistances R_{yy} and R_{xy} were measured in the linear regime upon passing an alternating electric current at a frequency of 888 Hz with an amplitude not exceeding 1 μA. The total electron density n_T in the quantum wells was calculated from the resistance R_{xy} measured in a magnetic field of $B = 0.5$ T for $\alpha = 0$. The electron mobility μ_y was calculated using the values of n_T and the resistance R_0 in zero magnetic field. The parameters of the samples are listed in Table 1.

Figure 2a shows the dependence of R_{yy}/R_0 on the magnetic field $B_z = B$ for the 46-nm-wide quantum well. One can see that MIS oscillations become manifested for $B_z > 0.05$ T. In the field range of $B_z > 0.5$ T, the MIS peak corresponding to $j = 1$ coexists with SdH oscillations. Figure 2b shows the fan diagrams for the two series of Landau levels demonstrating that the peaks of MIS oscillations appear when the energy levels belonging to the first and second subbands (E_N^S and E_N^{AS}, respectively) cross each other. The difference $\delta N = N^{AS} - N^S$ between the indices of the crossing Landau levels equals the peak number $j = \hbar\omega_{cz}/\Delta_{SAS}^0$, while the energy levels E_N^S and E_N^{AS} with the same indices never cross. Furthermore, the fan diagrams demonstrate that the crossings of the Landau levels for a given value of $j = \delta N$ occur at the same magnetic field values B_{zj}. These crossings are marked by vertical lines in Fig. 2b.

Figure 3a shows the experimental dependences of R_{yy}/R_0 on the inverse magnetic field $1/B_z$ for three different angles α. Analysis of these data indicates that MIS oscillations in tilted magnetic fields are no longer periodic in $1/B_z$. The $R_{yy}(1/B_z)/R_0$ dependences demonstrate that the peaks of MIS oscillations in a tilted magnetic field are shifted toward higher values of B_z in comparison to the case of $\alpha = 0$. This behavior was previously observed in a 56-nm-wide GaAs quantum well [18], but, owing to the small value of Δ_{SAS}^0, was not investigated in a broad range of magnetic fields. Formula (1) makes it possible to determine the energy splitting Δ_{SAS} from the magnetic-field position B_{zj} of the jth peak of MIS oscillations and, thus, to obtain the dependence $\Delta_{SAS}(B_x)$.

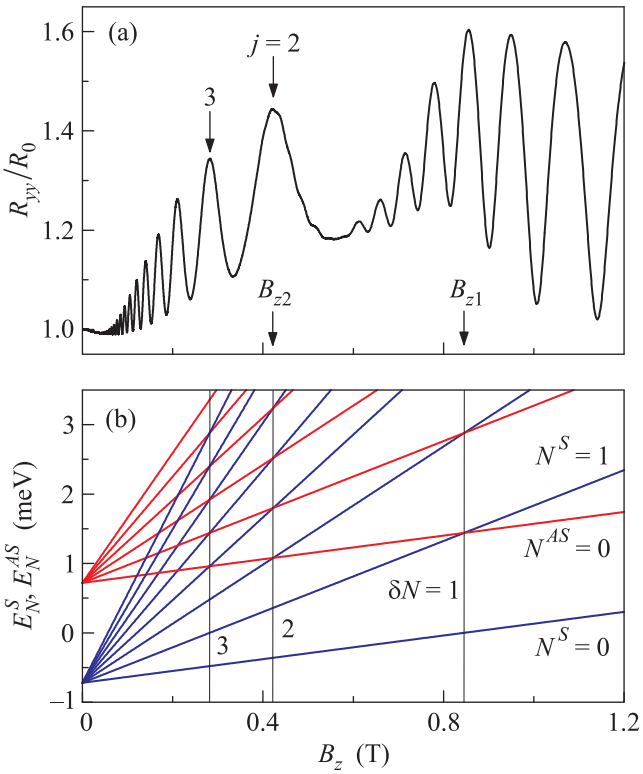

Fig. 2. (Color online) (a) Dependence $R_{yy}(B_z)/R_0$ at $T = 4.2$ K for sample no. 1. The tilt angle is $\alpha = 0$. Arrows indicate the peaks of MIS oscillations with numbers $j = 2$ and 3 and the values of B_{z1} and B_{z2}. (b) Dependences of E_N^S and E_N^{AS} on B_z for Landau levels in E^S and E^{AS} subbands, respectively, calculated by Eq. (3) with $\Delta_{SAS} = 1.44$ meV and $m^* = 0.068m_0$. Vertical lines show the values of B_z corresponding to the crossings of Landau levels with indices differing by $\delta N = 1$–3.

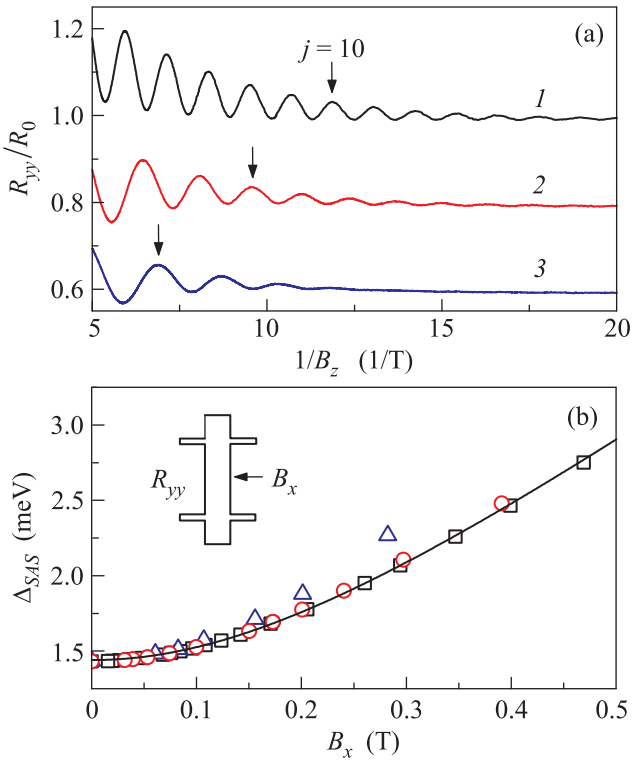

Fig. 3. (Color online) (a) Dependences $R_{yy}(1/B_z)/R_0$ for sample no. 1 at $T = 4.2$ K for tilt angles of $\alpha = 0°$, 63.1°, and 70.1°. Arrows indicate the MIS oscillation peak with the number $j = 10$. Curves *2* and *3* are shifted downward for clarity. (b) Dependences $\Delta_{SAS}(B_x)$ for sample no. 1. Triangles, circles, and squares show the values of Δ_{SAS} obtained from the positions of MIS oscillation peaks with numbers $j = 2$, 5, and 10, respectively. The solid line shows the result of calculation by Eq. (4) with $\Delta_{SAS}^0 = 1.44$ meV and $dk_F = 4.22$. The inset shows schematically the measurement scheme. The arrow shows the direction of B_x.

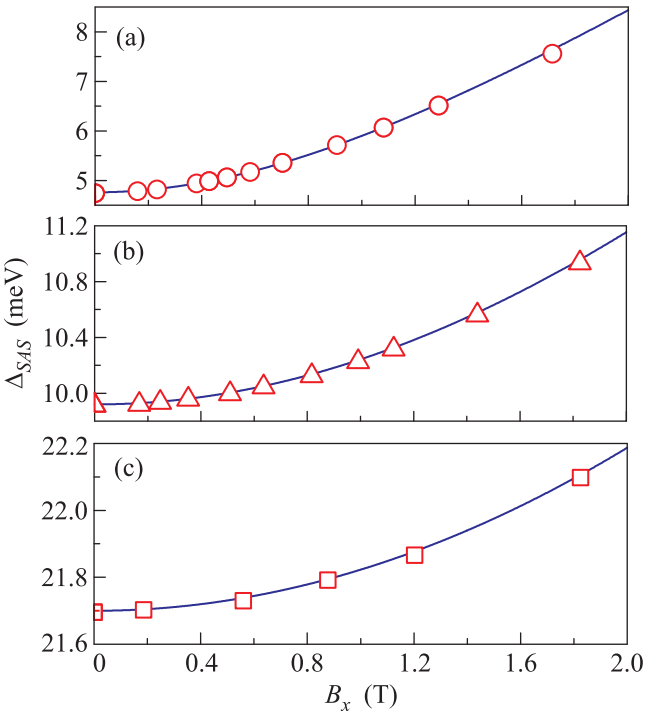

Fig. 4. (Color online) Dependences $\Delta_{SAS}(B_x)$ for samples nos. 2–4. Circles, triangles, and squares show the experimental values of Δ_{SAS} for quantum wells 36, 30, and 22 nm in width obtained from the positions of MIS oscillation peaks with numbers $j = 21$, 20, and 40, respectively. Solid lines show the results of calculations by Eq. (4) with (a) $\Delta_{SAS}^0 = 4.76$ meV and $dk_F = 2.92$, (b) $\Delta_{SAS}^0 = 9.92$ meV and $dk_F = 2.14$, and (c) $\Delta_{SAS}^0 = 21.7$ meV and $dk_F = 1.93$.

Under the condition $\hbar\omega_{cz} \ll \Delta_{SAS}^0$, electrons occupying Landau levels with high indices move semiclassically along trajectories corresponding to the symmetric, E^S, and antisymmetric, E^{AS}, states. For $\alpha = 0$, the semiclassical trajectories of electrons with the energy ε_F are represented in the quasimomentum space by concentric circles with the Fermi radii k_{FS} and k_{FAS}, whose areas are determined by the electron densities n_S and n_{AS} in the corresponding subbands. In this case, Δ_{SAS} is independent of k [1, 2]. An increase in B_x leads to an increase in the difference between the areas encircled by the trajectories of electrons in the symmetric and antisymmetric states and, thus, to an increase in Δ_{SAS}.

The experimental values of $\Delta_{SAS}(B_x)$ determined from the values of B_{zj} for $j = 2$, 5, and 10 are shown in Fig. 3b by triangles, circles, and squares, respectively. The solid line shows the dependence $\Delta_{SAS}(B_x)$ calculated according to Eq. (4) with the fitting parameter $dk_F = 4.22$. Good agreement between the calculated curve and experimental data is observed for MIS oscillation peaks with numbers $j > 10$. The deviation of the calculated values of Δ_{SAS} from the experimental ones for $j = 2$ and 5 indicates that the influence of B_z on the energy spectrum of electrons in these cases cannot be disregarded any more [18].

It should be noted that the value of the fitting parameter $dk_F = 4.22$ differs from the value $dk_F = 5.42$ obtained for sample no. 1 as the product of $(k_{FS} + k_{FAS})/2 = 1.62 \times 10^8$ m^{-1} and the spacing $d_\Psi = 33.4$ nm between the peaks of the wavefunctions $\Psi_{S\Gamma}$ and $\Psi_{AS\Gamma}$ (see Fig. 1b). Figure 4 shows the theoretical and experimental values of $\Delta_{SAS}(B_x)$ for quantum wells with the widths of 36, 30, and 22 nm. The semiclassical theory agrees well with experiment for all of them. However, as in the case of sample no. 1, there is no agreement between the values of the parameter dk_F obtained from

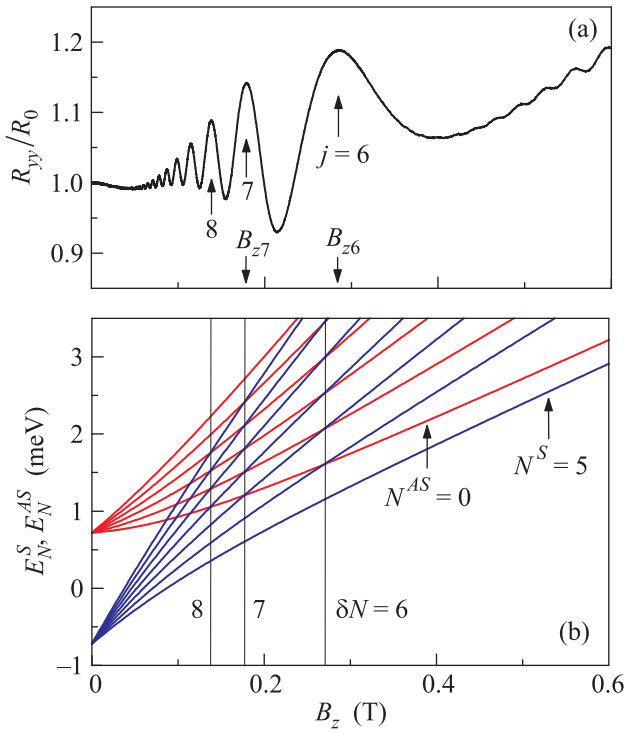

Fig. 5. (Color online) (a) Dependence $R_{yy}(B_z)/R_0$ at $T =$ 4.2 K for sample no. 1. The tilt angle is $\alpha \approx 59.9°$. Arrows indicate MIS oscillation peaks with numbers $j = 6$–8 and the values of B_{z6} and B_{z7}. (b) Dependences of E_N^S and E_N^{AS} on B_z for Landau levels in E^S and E^{AS} subbands, respectively, calculated by Eqs. (3) and (4) with $\Delta_{SAS}^0 = 1.44$ meV, $m^* = 0.068m_0$, and $dk_F = 4.22$. Vertical lines show the values of B_z corresponding to the crossings of Landau levels whose indices differ by $\delta N = 6$–8.

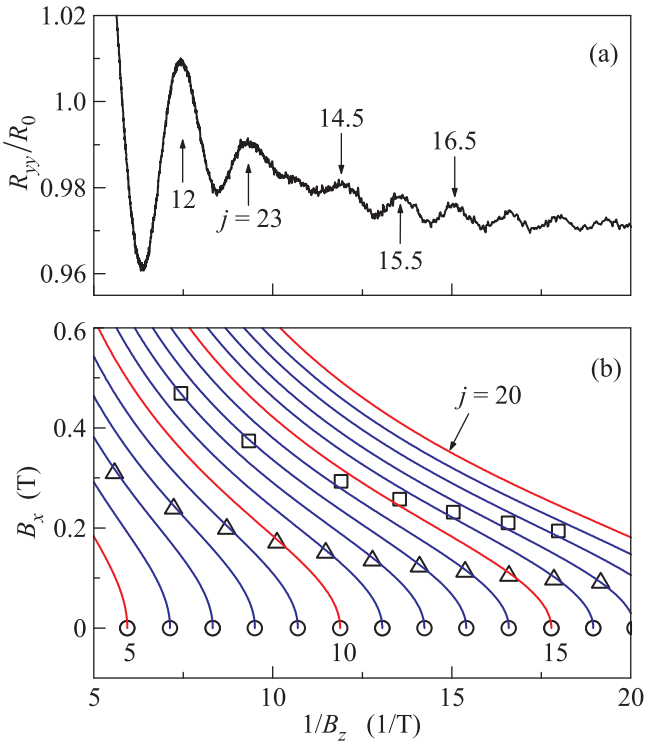

Fig. 6. (Color online) (a) Dependence $R_{yy}(B_z)/R_0$ at $T =$ 4.2 K for sample no. 1. The tilt angle is $\alpha \approx 74°$. Arrows indicate MIS oscillation peaks. (b) Solid lines show the positions of MIS oscillation peaks on the $(B_x, 1/B_z)$ plane for the quantum well with a width of $d_W = 46$ nm calculated by Eq. (4) with $\Delta_{SAS}^0 = 1.44$ meV and $dk_F = 4.22$ for $j = 5$–20. Circles, triangles, and squares show the experimental positions of MIS oscillation peaks for angles $\alpha =$ 0°, 59.9°, and 74.0°, respectively.

the fits for samples nos. 2–4 and those calculated as the product of $k_F = (k_{FS} + k_{FAS})/2$ and d_Ψ.

Figure 5a shows the dependence of R_{yy}/R_0 on the magnetic field B_z for the 46-nm-wide quantum well at the angle $\alpha \approx 60°$. Magnetointersubband oscillation peaks with numbers $j < 6$ are absent in this dependence. Figure 5b shows the fan diagrams for the two series of Landau levels calculated by Eq. (3). The dependence of Δ_{SAS} on B_x in a tilted magnetic field was taken into account according to Eq. (4) with the fitting parameter $dk_F = 4.22$. The absence of MIS oscillation peaks with $j < 6$ results from the dependence $\Delta_{SAS}(B_x)$. Because of this dependence, there are no crossings of Landau levels with $\delta N < 6$ in the case of $\alpha \approx 60°$, in contrast to $\alpha = 0$. Meanwhile, according to the fan diagrams in Fig. 5b, all crossings of Landau levels of different subbands with $\delta N > 5$ occur at the same magnetic field, as in the case of $\alpha = 0$. These crossings are marked with vertical lines in this figure. However, the $j = 6$ peak is shifted to higher fields from that where crossings with $\delta N = 6$ take place. The reason is that Eq. (4) is valid only for $J > 10$ (Fig. 3b).

Figure 6a shows the dependence $R_{yy}(1/B_z)/R_0$ for the angle $\alpha \approx 74°$. One can see that the phase of MIS oscillations is broken between peak numbers $j = 13$ and 14. For this angle, the phase of oscillations changes by π for peaks with $j > 13$.This behavior of MIS oscillations in tilted magnetic fields was not observed previously [18, 20]. The phase of MIS oscillations is broken in the magnetic-field range where $\hbar\omega_{cz} \ll \Delta_{SAS}^0$ and, thus, Eq. (4) is valid. In this situation, only a smooth shift of the MIS oscillation peaks toward higher values of B_z, which results from the dependence of Δ_{SAS} on B_x, should be observed. The phase break of MIS oscillations was also observed for the 36-nm-wide quantum well for tilt angles exceeding 85° and was not observed in narrower quantum wells.

Using Eq. (4) with the parameter $dk_F = 4.22$, we calculated the dependences $B_{xj}(1/B_z)$ for MIS oscillation peaks with numbers $j > 5$. The results are plotted

by solid lines in Fig. 6b, where the positions of MIS oscillation peaks for tilt angles of $\alpha =$ (circles) 0°, (triangles) 59.9°, and (squares) 74.0° are shown. For angles $\alpha < 72°$, all peak positions fall on the calculated dependences, as seen in Fig. 6b for angle $\alpha = 59.9°$. For angles $\alpha > 72°$, MIS oscillation peak positions before the phase-break point also fall on the calculated dependences; however, they occur between the calculated curves after the phase break. This means that MIS oscillation peaks after the phase-break point are described by half-integer values of j. In other words, MIS oscillations change their phase by π after the break point.

Speculatively, the observed beats of MIS oscillations might be caused by Zeeman splitting, which increases with the angle α in the range of fields B_z where the beats occur. However, the magnitude of this splitting depends linearly on B and, therefore, it should lead only to the splitting of MIS oscillation peaks rather than to beats [23]. In addition, we observe no effect of Zeeman splitting on SdH oscillations in magnetic fields of $B_z \sim 2$ T, which allows us to exclude this factor from consideration. Since the beats of MIS oscillations are observed in the range of fields B_z where SdH oscillations are already suppressed, they can result only from the crossings of Landau levels. That is, with increasing α, one series of Landau level crossings characterized by numbers j is split into two series, which leads to MIS oscillations with close periods and, thus, to their beats. It was shown in [16, 20, 24] that the crossings of Landau levels with a given difference $\delta N = j$ of level indices at large angles α occur at different magnetic fields B_z, rather than at the same value B_{zj}. We believe that this transformation of crossings causes the beats of MIS oscillations.

To summarize, we have shown that the experimental dependences $\Delta_{SAS}(B_x)$ measured under the conditions $\hbar\omega_{cz} \ll \Delta_{SAS}$ and $(\hbar/eB_x)^{1/2} > d/2$ in 22- to 46-nm-wide quantum wells with two populated subbands E^S and E^{AS} are well described by Eq. (4) with a single fitting parameter dk_F. In addition, we have demonstrated that the lack of MIS oscillation peaks with small numbers in tilted magnetic fields is well described by Eqs. (3) and (4). We have found that beats take place in MIS oscillations in 46-nm and 36-nm quantum wells recorded for magnetic-field tilt angles $\alpha > 72°$ and 85°, respectively. The theoretical interpretation of this unexpected behavior of MIS oscillations is currently absent.

We are grateful to Alexei Nenashev for fruitful discussions of the experimental results.

This work was supported by the Russian Foundation for Basic Research (project no. 16-02-00592) and the Division of Materials Research, US National Science Foundation (grant no. 1702594).

REFERENCES

1. G. S. Boebinger, A. Passner, L. N. Pfeiffer, and K. W. West, Phys. Rev. B **43**, 12673(R) (1991).
2. J. Hu and A. H. MacDonald, Phys. Rev. B **46**, 12554 (1992).
3. V. M. Polyanovskii, Sov. Phys. Semicond. **22**, 1408 (1988).
4. D. R. Leadley, R. Fletcher, R. J. Nicholas, F. Tao, C. T. Foxon, and J. J. Harris, Phys. Rev. B **46**, 12439 (1992).
5. M. E. Raikh and T. V. Shahbazyan, Phys. Rev. B **49**, 5531 (1994).
6. O. E. Raichev, Phys. Rev. B **78**, 125304 (2008).
7. A. A. Bykov, D. R. Islamov, A. V. Goran, and A. I. Toropov, JETP Lett. **87**, 477 (2008).
8. N. C. Mamani, G. M. Gusev, T. E. Lamas, A. K. Bakarov, and O. E. Raichev, Phys. Rev. B **77**, 205327 (2008).
9. A. V. Goran, A. A. Bykov, A. I. Toropov, and S. A. Vitkalov, Phys. Rev. B **80**, 193305 (2009).
10. A. A. Bykov, A. V. Goran, and S. A. Vitkalov, Phys. Rev. B **81**, 155322 (2010).
11. S. Wiedmann, G. M. Gusev, O. E. Raichev, A. K. Bakarov, and J. C. Portal, Phys. Rev. B **82**, 165333 (2010).
12. A. A. Bykov, JETP Lett. **100**, 786 (2015).
13. S. Dietrich, J. Kanter, W. Mayer, S. Vitkalov, D. V. Dmitriev, and A. A. Bykov, Phys. Rev. B **92**, 155411 (2015).
14. A. A. Bykov, A. V. Goran, and A. K. Bakarov, J. Phys. D: Appl. Phys. **51**, 28LT01 (2018).
15. I. L. Drichko, I. Yu. Smirnov, M. O. Nestoklon, A. V. Suslov, D. Kamburov, K. W. Baldwin, L. N. Pfeiffer, K. W. West, and L. E. Golub, Phys. Rev. B **97**, 075427 (2018).
16. N. Kumada, K. Iwata, K. Tagashira, Y. Shimoda, K. Muraki, Y. Hirayama, and A. Sawada, Phys. Rev. B **77**, 155324 (2008).
17. I. A. Larkin, S. Ujevic, S. Wiedmann, N. Mamani, G. M. Gusev, A. K. Bakarov, and J. C. Portal, J. Phys.: Conf. Ser. **456**, 012025 (2013).
18. W. Mayer, J. Kanter, J. Shabani, S. Vitkalov, A. K. Bakarov, and A. A. Bykov, Phys. Rev. B **93**, 115309 (2016).
19. W. Mayer, S. Vitkalov, and A. A. Bykov, Phys. Rev. B **93**, 245436 (2016).
20. W. Mayer, S. Vitkalov, and A. A. Bykov, Phys. Rev. B **96**, 045436 (2017).
21. K.-J. Friedland, R. Hey, H. Kostial, R. Klann, and K. Ploog, Phys. Rev. Lett. **77**, 4616 (1996).
22. D. V. Dmitriev, I. S. Strygin, A. A. Bykov, S. Dietrich, and S. A. Vitkalov, JETP Lett. **95**, 420 (2012).
23. S. A. Tarasenko, N. S. Averkiev, JETP Lett. **75**, 552 (2002).
24. Yu. G. Arapov, V. N. Neverov, G. I. Harus, N. G. Shelushinina, and M. Ya. Yakunin, Low Temp. Phys. **35**, 133 (2009).

Translated by M. Skorikov

SPELL: OK